Journal of Quantitative Spectroscopy & Radiative Transfer 347 (2025) 109690

Contents lists available at ScienceDirect

Journal of Quantitative Spectroscopy and Radiative Transfer

journal homepage: www.elsevier.com/locate/jqsrt

High-resolution (8–16 MHz) rovibrational absorption spectra of low-pressure methanol, ethanol, isoprene, and dimethyl sulfide at 700–1500 cm^{-1} measured via dual-comb spectroscopy

D. Konnov, A. Muraviev, K.L. Vodopyanov *

CREOL, The College of Optics and Photonics, University of Central Florida, Orlando, FL, USA

ARTICLE INFO

Keywords:
Methanol
Ethanol
Isoprene
Dimethylsulfide
Absorption cross sections
Dual-comb spectroscopy

ABSTRACT

We employ dual-comb spectroscopy, a state-of-the-art technique that utilizes a pair of broadband mutually coherent laser frequency combs, to acquire high spectral resolution mid-infrared absorption spectra of molecules relevant to terrestrial and exoplanetary atmospheres. We have recorded room-temperature spectra of low-pressure methanol, ethanol, isoprene, and dimethyl sulfide in the 700–1500 cm^{-1} (6.7–14.3 μm) range with the resolution down to 8 MHz (2.7×10^{-4} cm^{-1}) and with the absolute frequency accuracy of 10^{-7} cm^{-1}, limited by the accuracy of a rubidium atomic clock. To date, this dataset represents the most comprehensive longwave infrared absorption spectra of these four molecules.

1. Introduction

High-resolution molecular absorption spectra in the fingerprint region (500–1500 cm^{-1}) are crucial for a wide range of applications, including remote sensing, environmental monitoring, medical diagnostics, planetary science, exobiology, and fundamental spectroscopy. Comprehensive databases of absorption line positions and intensities enable improved detection and differentiation within complex gas mixtures, as well as accurate simulations leading to assignment of quantum transitions and the construction of effective Hamiltonians. These, in turn, allow for the generation of line lists capable of predicting molecular spectral behavior under varying temperatures and pressures. Acquiring spectra at low pressures, where absorption lines are primarily Doppler-broadened, is particularly important for molecules that exhibit highly congested and overlapping vibrational bands.

Methanol (CH_3OH). Methanol, the simplest alcohol, is a key building block of complex organic compounds essential to life and is widely studied for its significance in astrophysical and atmospheric contexts. Among the four molecules examined in this study, it is the most widely characterized. Xu et al. [1] conducted extensive Fourier transform infrared (FTIR) spectrometer measurements of methanol in the 960–1080 cm^{-1} range. The spectral resolution of 0.002 cm^{-1} (60 MHz) at 0.10 Torr pressure allowed line assignments in the spectrum of CH_3OH, significantly expanding the catalog of weak subbands. These included high-K and torsionally excited subbands of the ν_8 CO-stretching mode, as well as torsional combination bands involving the ν_7 in-plane CH_3 rocking, ν_6 OH bending, and ν_5 symmetric CH_3 deformation modes. Additionally, this work improved the spectroscopic understanding of numerous weak absorption features occurring in the spectral windows between the stronger ν_8 transitions. These data are now part of the HITRAN2020 database [2]. While the spectral resolution in [1] was sufficient to reveal numerous previously unobserved features of methanol, the present work, provides opportunities for further refinement of the methanol spectrum. These results support its inclusion in the forthcoming HITRAN24 database as a cross-section spectrum and lay the groundwork for the development of an improved line list in future HITRAN editions.

Ethanol (C_2H_5OH). Ethanol is a key molecule in astro- and prebiotic chemistry. Detection of ethanol in the interstellar medium confirms that relatively complex organic molecules can form in space under cold low-density conditions. This serves as evidence of chemical pathways that could lead towards amino acids, sugars and nucleobases. Presence of ethanol alongside other complex organics increases the plausibility of abiotic synthesis of life's building blocks [3]. Interpreting vibrational spectra of ethanol involves several challenges. In comparison with methanol, ethanol has an additional CH_2 group and 21 vibrational modes, resulting in more congested absorption bands, some of which can overlap, making it difficult to resolve individual lines. Also, ethanol

* Corresponding author.
E-mail address: vodopyanov@creol.ucf.edu (K.L. Vodopyanov).

https://doi.org/10.1016/j.jqsrt.2025.109690
Received 17 June 2025; Received in revised form 23 September 2025; Accepted 24 September 2025
Available online 26 September 2025

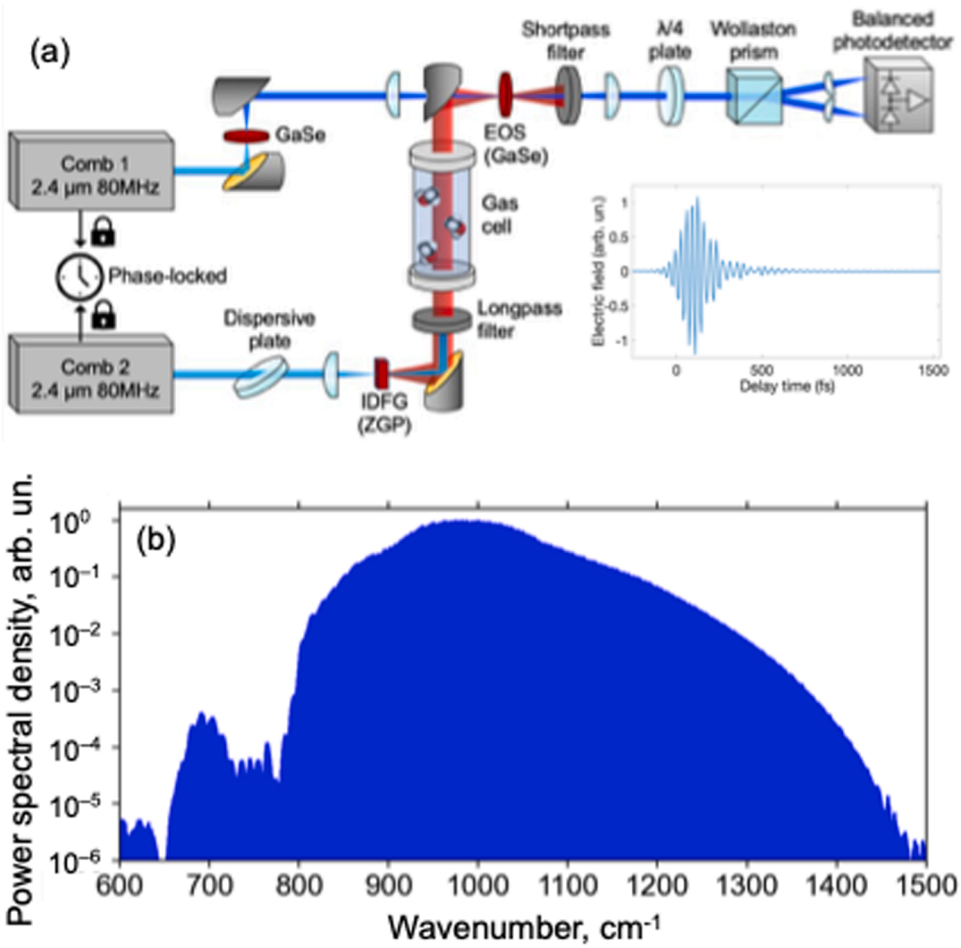

Fig. 1. Schematic of the dual-comb spectroscopy setup. (a) Two phase-locked Cr:ZnS laser combs with central wavelength 2.35 μm are used as a driving source. The output of one of the laser combs is downconverted via IDFG in a ZGP nonlinear crystal to produce a broadband MIR comb, while the second Cr:ZnS laser comb is converted to the NIR via second harmonic generation (SHG) and is used as a source of gate pulses. The inset shows a typical measured electric field waveform. (b) The MIR comb spectrum spanning 7.1–14.3 μm (700–1500 cm^{-1}).

has conformational flexibility, so it can adopt anti (trans) and gauche forms that feature slightly different rovibrational signatures, so the observed spectrum is a population-weighted average. Doppler-broadened absorption spectrum for ethanol in the fingerprint region carries out especially rich and scientifically valuable information. The currently available spectroscopic data for ethanol in the long-wave infrared region is limited to low-resolution measurements (0.11 cm^{-1}) conducted at atmospheric pressure [4]. This experimental dataset, published over two decades ago, remains the primary reference for ethanol in this spectral range. However, its limited spectral resolution prevents the accurate resolution of individual lines within complex vibrational bands, making the development of reliable line lists infeasible. Notably, Ding et al. [5] employed a rapid-scan external-cavity quantum cascade laser with a linewidth of 100 MHz (0.0033 cm^{-1}) in combination with a shock tube to measure absorption cross-section profiles in the C–O stretching band of methanol and ethanol, covering the 930–1170 cm^{-1} region. Their experiments were conducted at elevated temperatures (up to 1300 K) and pressures (up to 3.3 atm), revealing the appearance of hot bands and high-J rovibrational transitions. These results contribute significantly to the development of high-temperature spectroscopic databases.

Isoprene (C_5H_8). Isoprene is the most abundantly emitted hydrocarbon by vegetation and plays an important role in atmospheric chemistry through ozone and cloud formation. In the exoplanetary science, isoprene can be a perfect candidate as a biosignature due to its biological specificity, unlike some smaller organic molecules that can be abiotic, so detection of it might indicate active biogenic processes [6,7]. It is also considered an important biomarker in human breath [8,9]. Isoprene is the largest molecule studied in this paper; it has 13 atoms giving in total 33 vibrational modes, with most of them being IR active. It has two conjugated double bonds, a diene, giving a delocalized π system resulting in the coupled $C = C$ stretch modes making it harder for spectral interpretation. High-resolution spectral data can help to isolate these modes of the conjugated diene system. The CH_3 group in the isoprene has a rigid bond within the conjugated system hindering the contribution from the methyl group internal rotation, which usually couples with vibrational modes and introduces band broadening and splitting of absorption lines. On the other hand, because of the multiple CH stretching and bending modes that are mixed and close in frequency, the absorbance spectrum features crowded and overlapped absorption bands, which easily blend when the collisional line broadening is just a few times higher than the Doppler one. Brauer et al. [10] reported absorption cross sections and integrated band intensities for isoprene in the 600–6500 cm^{-1} region. The pressure-broadened (1 atm, N_2 buffer gas) spectra were recorded at 278, 298, and 323 K at 0.112 cm^{-1} resolution, using a Bruker IFS 66v/S FTIR spectrometer. The authors have modified some vibrational assignments of isoprene assuming the planar s-trans configuration, partially in agreement with prior works. However, weak absorption features occurring in the vicinity of the two strong C-type bands (ν_{27} and ν_{28}) at 906.3 and 893.8 cm^{-1}, were not resolved in this work.

DMS ($(CH_3)_2S$). DMS is the most abundant sulfur-containing organic

compound emitted into Earth's atmosphere, which is mainly produced by marine phytoplankton. It plays a significant role in the sulfur cycling and cloud formation, so this molecule is particularly important for atmospheric chemistry and environmental science. Moreover, DMS is a known biomarker detected in breath which might indicate liver dysfunction and halitosis [11,12]. Similar to isoprene, DMS has minimal abiotic sources which makes it a compelling biosignature candidate [6]. It stands out among biosignature gases for ocean-bearing exoplanets or reduced atmospheres. DMS has 9 atoms resulting in 21 vibrational modes. In comparison with ethanol or isoprene, vibrational modes for DMS have minimal contribution from the conformational complexity. However, it has methyl group internal rotation effects coming from two CH_3 groups that have a low torsion barrier resulting in a quasi-free rotation. Due to the multiple CH_3 torsional modes and coupled internal rotations between these two methyl groups, vibrational bands in the fingerprint region for DMS experience a complicated splitting and broadening making high-resolution low-pressure spectroscopic studies particularly important. Using a high-resolution FTIR spectrometer, Jabri et al. recorded a room-temperature rovibrational spectrum of the ν_{14} CH_3-bending mode of DMS in the 900–1075 cm^{-1} spectral region with 0.003 cm^{-1} (90 MHz) spectral resolution and provided line assignments [13]. Additional experiments performed by the authors with jet-cooled molecules and a tunable quantum cascade laser were critical to these assignments. Overall, 1119 transitions from both jet-cooled and room temperature experiments were assigned and included in a global fit with $J \leq 29$. A total of 9 rovibrational parameters including pure rotational constants as well as quartic centrifugal distortion constants were determined with high accuracy [13].

In this work, we present a broadband spectroscopic study of gaseous methanol, ethanol, isoprene, and dimethyl sulfide over the range 700–1500 cm^{-1} with spectral resolution down to 8 MHz (0.00027 cm^{-1}), enabled by the dual-comb laser spectroscopy.

2. Experimental setup

The *dual-comb spectroscopy* (DCS) method, a subtype of Fourier transform spectroscopy exploits the spatial and temporal coherence of broadband optical frequency combs and provides significantly improved performance over classical FTIR spectrometers in terms of achievable spectral resolution and signal-to-noise characteristics [14,15]. DCS is based on the superposition of two mutually coherent laser frequency combs, where the second comb has a small offset in pulse repetition rate and effectively acts as a time-delayed second arm in a Michelson interferometer. DCS is a powerful technique that allows high-precision spectroscopic measurements with the frequency scale referenced to an atomic clock [15].

As a detection method for DCS, we employed electro-optic sampling (EOS), a state-of-the-art technique enabling the full characterization of electric-field waveforms in both amplitude and phase [16–18]. Here, the electric field, rather than the intensity, of the mid-infrared (MIR) wave, which carries the spectral information of the absorbing molecules, is measured through its interaction with a near-infrared (NIR) 'gate' pulse. When the MIR and NIR pulses temporally and spatially overlap within an electro-optic crystal, the MIR field induces a polarization change in the gate pulse, which is detected using a balanced NIR photodetector. The main advantage of using EOS lies in the ability to do measurements in the longwave infrared range (MIR to terahertz) eliminating the need for cryogenically cooled detectors. This enabled getting the signal-to-noise ratio of up to 10,000 with respect to the strongest absorption peaks in our MIR absorption spectra with MHz scale resolution.

A schematic of the dual-comb spectroscopy setup is shown in Fig. 1a. As a driving source, we used a pair of mutually phase-locked frequency combs based on mode-locked Cr:ZnS lasers with center wavelength 2.35 μm, average power 3 W, pulse duration 30 fs, and the pulse repetition rate f_{rep}=80 MHz, referenced to a rubidium (Rb) atomic clock. The output of one of the laser combs was downconverted via intrapulse difference frequency generation (IDFG) in a ZnGeP2 (ZGP) nonlinear

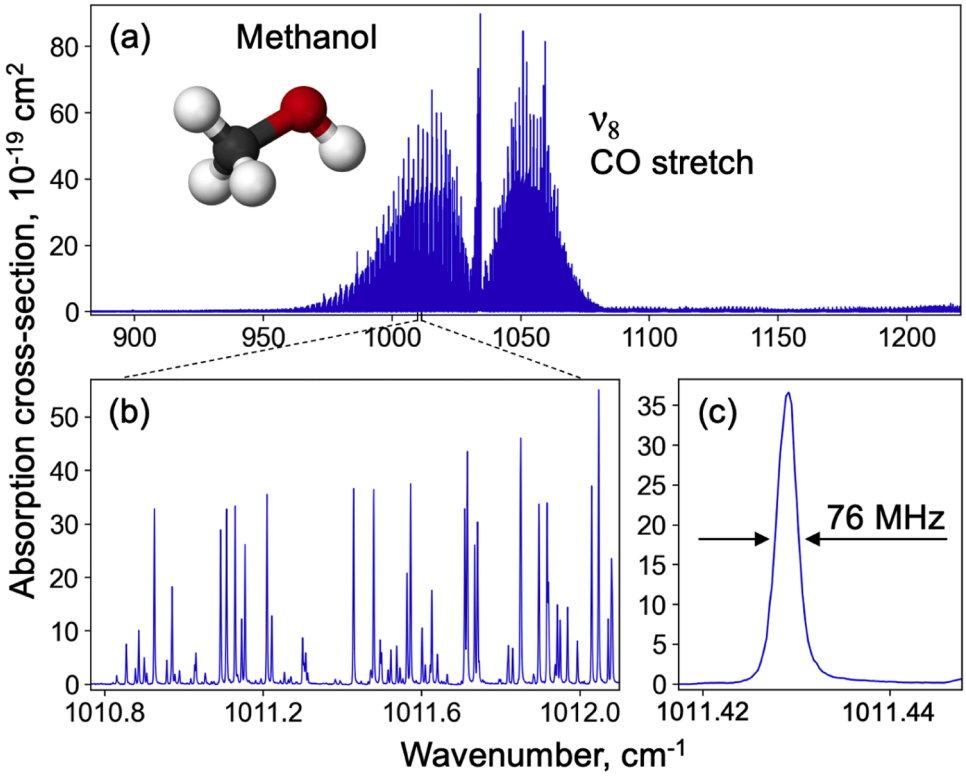

Fig. 2. (a) Absorption cross-section spectrum of methanol. (b) Magnified view highlighting the fine structure within the spectrum. (c) Detailed zoom-in showing an individual absorption line.

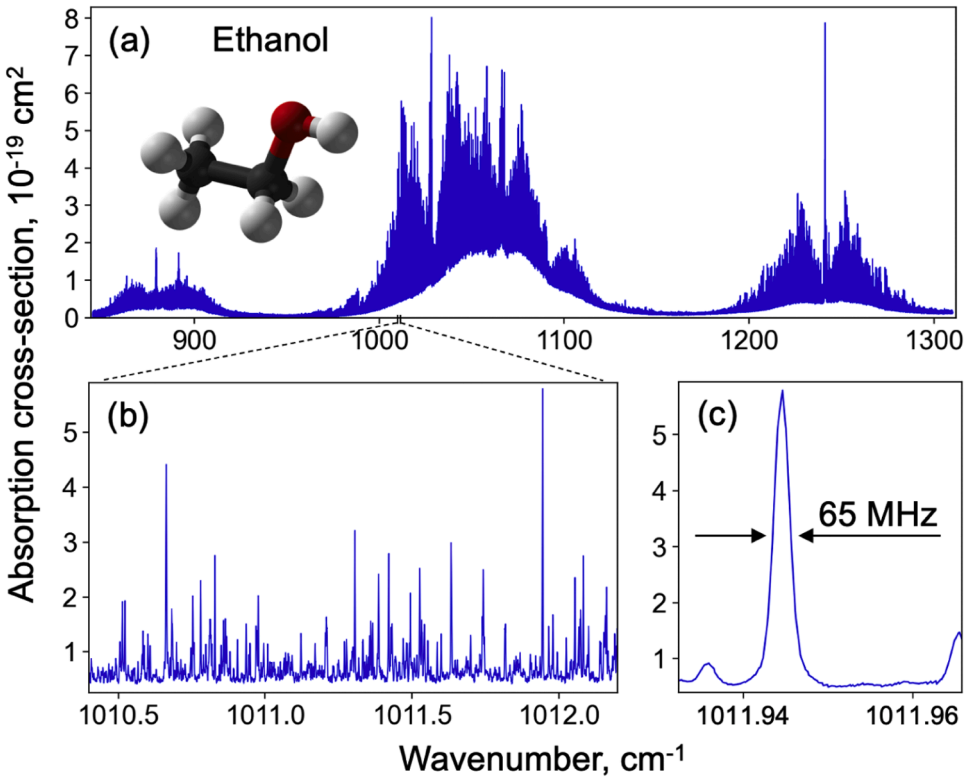

Fig. 3. (a) Absorption cross-section spectrum of ethanol. (b) Magnified view highlighting the fine structure within the spectrum. (c) Detailed zoom-in showing an individual absorption line.

crystal to produce a long-wave comb spanning 6.7–12.5 μm (800–1500 cm^{-1}, see Fig. 1b) [19]. Alternatively, to access longer wavelengths (up to 14.3 μm (700 cm^{-1}), we used a GaSe nonlinear crystal [20]. In our EOS detection method, the polarization change of the NIR gate pulse was measured by an ellipsometry setup containing a quarter-wavelength ($\lambda/4$) plate, a Wollaston prism, and a balanced NIR photodetector. For the NIR gate, we used the second Cr:ZnS laser comb that was converted to its second harmonic (Fig. 1a) [18].

The output of the balanced NIR detector, consisting of periodic interferograms repeating at a period of $1/\Delta f_{rep}$, where Δf_{rep} is the pulse repetition rate offset between the combs, was digitized using a 16-bit analog-to-digital converter (AlazarTech ATS9626) with consequent fast Fourier transform (FFT) algorithm to obtain the spectrum. In each single spectral measurement, we obtain about 260,000 comb-line-resolved spectral points with the comb-line spacing of f_{rep}=80 MHz. To achieve the spectral resolution finer than the comb-line spacing, we interleaved several comb-line-resolved DCS spectra by gradual shifting the combs [21] with the resulting data point spacing in the combined spectrum of 8–16 MHz, which was smaller than the Doppler linewidth of the molecules studied. Due to the low pressure and high resolution, the spectral lines of the interfering molecules, such as H_2O and CO_2 present in the gas mixture, practically did not affect the spectra of studied molecules. The resulting spectrum was normalized using a reference spectrum recorded with an empty gas cell. Absorption cross-section plots were generated based on the known optical path length, sample concentration, temperature, and pressure. To mitigate residual low-frequency baseline variations, the measured spectrum with artificially reduced resolution was compared to the established low-resolution reference spectrum, such as the PNNL database [4], and appropriate corrections were applied to the baseline. For the strongest absorption peaks, the spectral signal-to-noise ratio (SNR) reached 10^4 in our experiments – mostly limited by weak fast baseline fluctuations due to uncompensated etalon effects.

Gas samples of all four analytes —methanol, ethanol, isoprene, and dimethyl sulfide (DMS)—were evaporated from its liquid state into a pre-evacuated gas cell. The temperature within the cell was maintained at 296 K. Typically, to obtain a desired signal-to-noise ratio, we coherently averaged from $N = 50{,}000$ to $N = 1000{,}000$ interferograms. With a repetition rate offset between the two combs of $\Delta f_{rep} = 69$ Hz, corresponding to the period between interferograms of 14 ms, this resulted in a measurement time for one spectrum from 12 to 240 min, correspondingly.

3. Results

3.1. Methanol (CH_3OH)

The absorption spectrum of pure gaseous methanol was measured using a 44.5 cm-long gas cell at a pressure of 0.81 mbar. At this pressure, collisional broadening contributed to less than 5 % to the total linewidth, ensuring that the absorption features remained close to the Doppler-limit. The cell length was selected to yield the absorbance A of the strongest peaks in the range of 1 to 5, which optimizes the signal-to-noise ratio while avoiding nonlinear effects due to absorption peak saturation. (Here absorbance is defined as $A = -\ln(I/I_0)$, where I is the transmitted intensity with the filled cell, and I_0 is the transmitted intensity with the empty cell.) With the nominal comb line spacing of 80 MHz, we achieved the data point spacing of 8 MHz by interleaving 10 spectra measured with incrementally frequency shifted combs. We coherently averaged $N = 50{,}000$ interferograms for each spectrum. The absorption cross-section spectrum of methanol is shown in Fig. 2. Here, we observe the ν_8 vibrational band of methanol, which dominates in the 10 μm region of the Mid-IR. This is also the strongest and most distinctive absorption band in the vapor-phase methanol. This absorption band, centered around 1033 cm^{-1}, has clear identifications of the P, Q, and R branches, and it corresponds to the fundamental CO bond stretch mode in methanol as it is assigned in [1].

Several studies have reported sub-Doppler saturation-dip spectra of

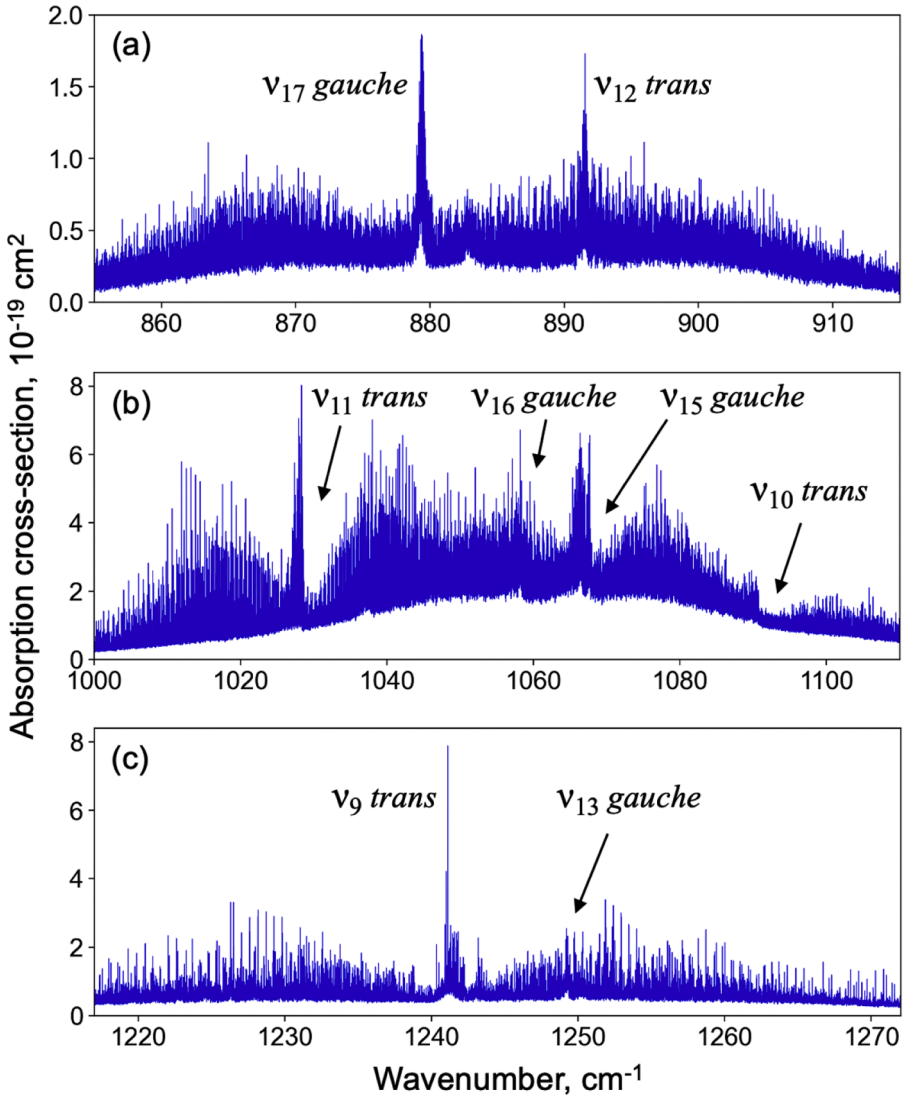

Fig. 4. Portions of absorption cross-section spectrum of ethanol with mode assignments.

the ν_8 band in methane with sub-MHz resolution, either using a dual-mode CO_2 laser/microwave sideband spectrometer [22] or a tunable, ultra-narrow linewidth quantum cascade laser stabilized via a NIR frequency comb, itself referenced to an ultra-stable laser [23,24]. A comparison of our results with the most advanced recent measurements of [24], covering a 1.4 GHz (0.047 cm^{-1}) range near 971 cm^{-1}, shows that the central positions of our Doppler-broadened peaks deviate by less than 3 MHz (that is much less than the Doppler linewidth) from the Doppler-free peaks shown in Fig. 2(a) of [24]. This is consistent with the nominal resolution of our DCS system.

3.2. Ethanol (C_2H_5OH)

The absorption cross-section spectrum of gaseous ethanol, shown in Fig. 3, was measured at a pressure of $p = 0.5$ mbar and the optical cavity length of 238 cm. Zoomed-in portions of the spectrum with assignment of fundamental vibrational modes are shown in Fig. 4. The spectrum was acquired by interleaving 10 gradually shifted comb-mode-resolved spectra resulting in the data point spacing of 8 MHz, which allowed resolving manifolds of narrow absorption features. We coherently averaged $N = 1000{,}000$ interferograms for each shifted spectrum. A significant enhancement in spectral resolution in comparison to the state-of-the-art [4] allowed resolving fine structure with manifolds of peaks as narrow as 65 MHz. The obtained high-resolution spectra may facilitate the future modeling of multiple hybrid a/b-type rovibrational bands in ethanol due to asymmetric CO/CC stretching and COH bending vibrations near 1000 cm^{-1} [25].

On the acquired spectrum, we observed absorption bands of at least eight fundamental vibrational modes of ethanol. It worth mentioning that the abundance of the *trans* conformer of ethanol present at ambient temperature is 40 ± 1 % according to the [26], while the *gauche* form takes around 60 %. Here we used mode assignments and descriptions of molecular motion involved in the fundamental vibration that was predicted in [26] by comparing experimental spectra and performing the *ab initio* calculations. On this spectrum, we identified four fundamental bands for each of the conformers which are in excellent agreement with [26].

On the lower frequency end (Fig. 4a), the absorption band near 879 cm^{-1} is given by the ν_{17} mode of the *gauche* ethanol corresponding to the CC stretching. Here we also observed a weaker contribution of the ν_{12} mode of *trans* ethanol given by CH_3 rocking near 892 cm^{-1}. Both of these fundamental vibrational modes have hybrid a/b-type (~2:1 ratio) absorption bands.

In the region between 1000 and 1100 cm^{-1} (Fig. 4b), we identified four vibrational modes. There are three modes of a similar strength. One of them is the ν_{11} mode of the *trans* ethanol which is given by a CC

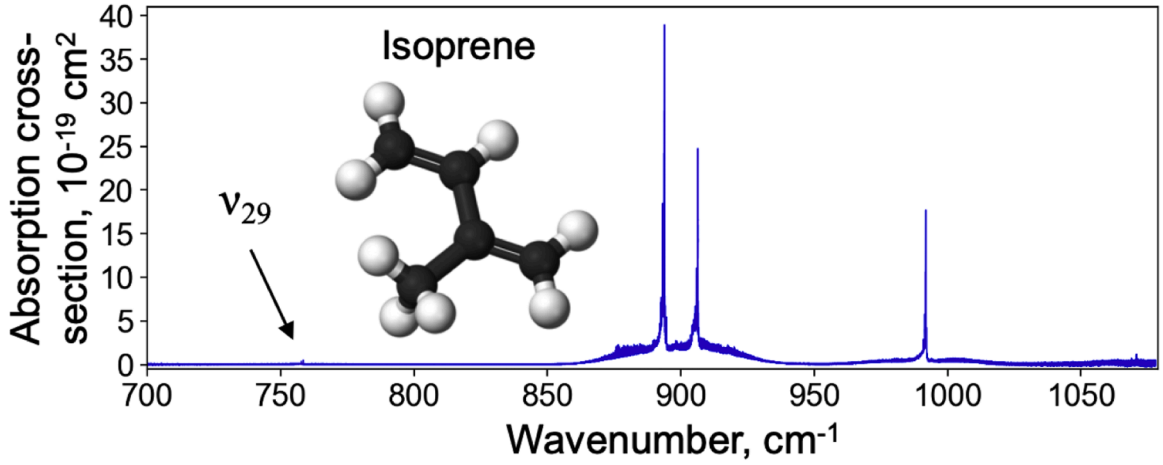

Fig. 5. Overview absorption cross-section spectrum of isoprene at $p = 4$ mbar.

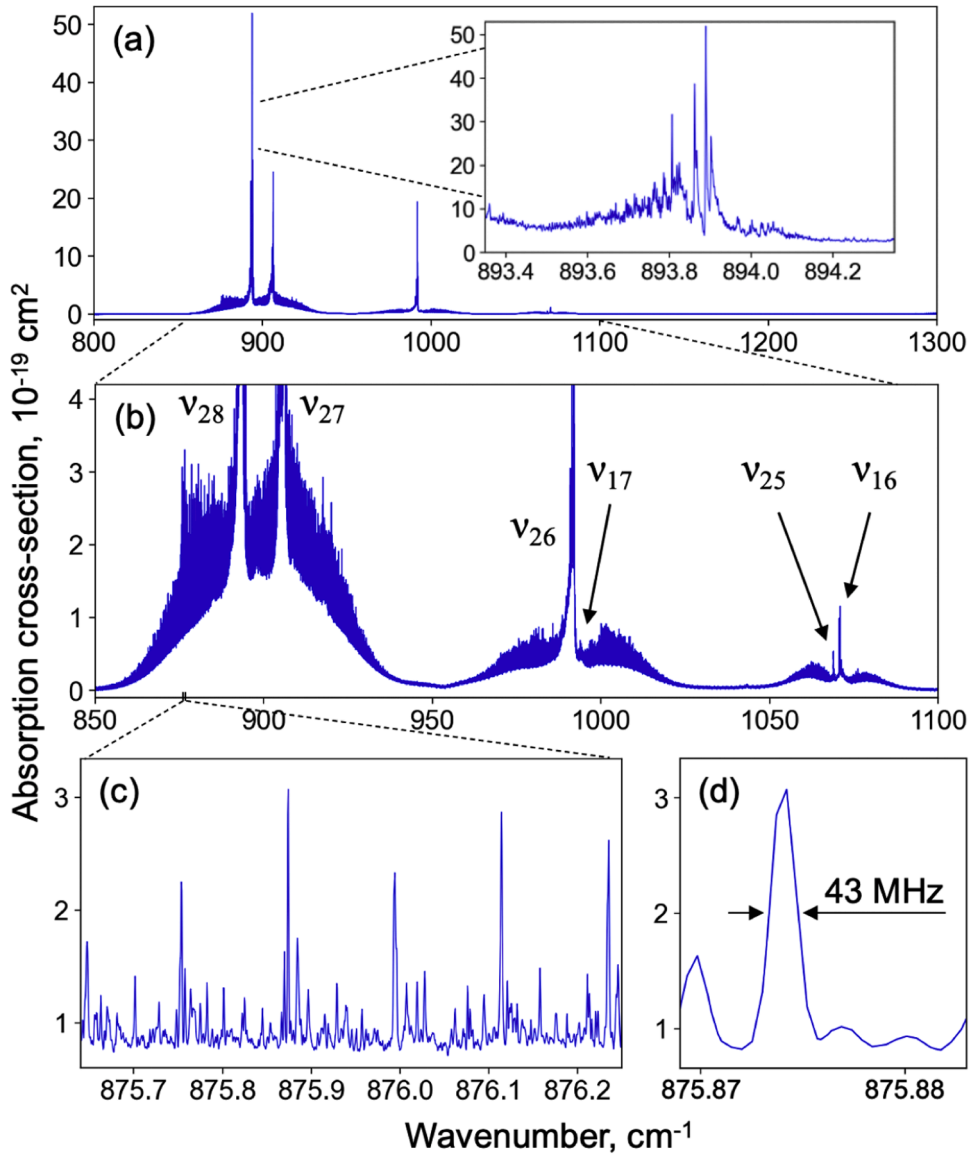

Fig. 6. (a) Absorption cross-section spectrum of isoprene at low pressure ($p = 0.185$ mbar). The inset highlights the structure of the strongest peak at 894 cm^{-1}. (b) Vertically expanded view of the spectrum. (c) Magnified portion revealing the fine spectral structure. (d) Further zoom-in showing an individual absorption line.

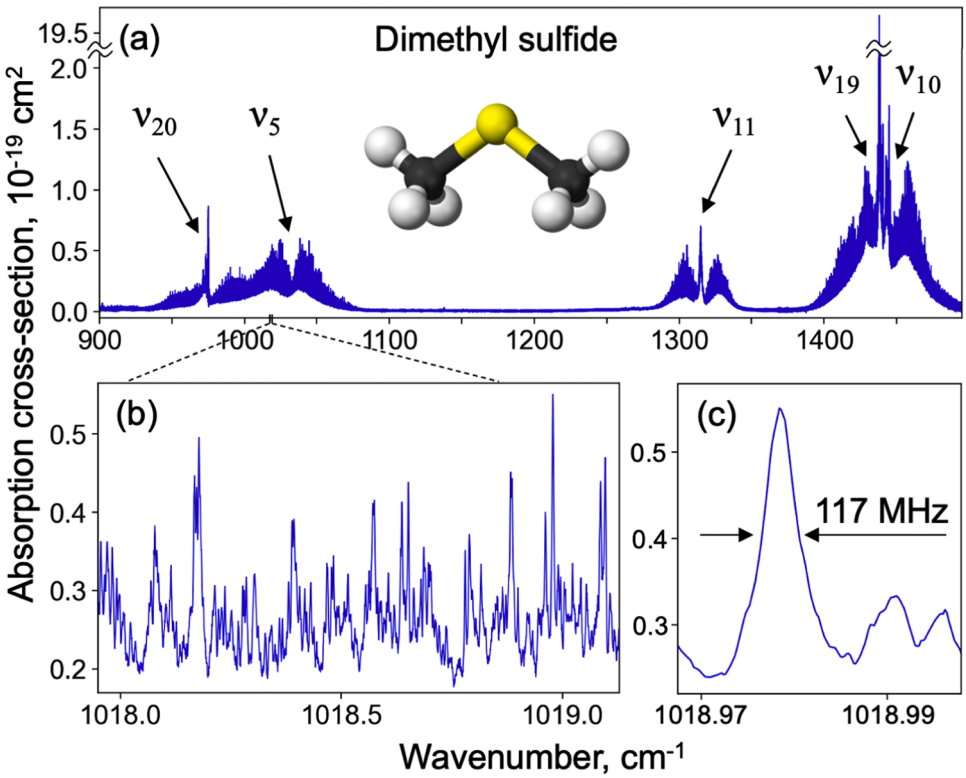

Fig. 7. (a) Absorption cross-section spectrum of DMS. (b) Magnified view highlighting the fine structure within the spectrum. (c) Detailed zoom-in showing an individual absorption line.

stretch vibration and centered near 1027 cm^{-1}. The other two strong modes are for the *gauche* ethanol, which are ν_{16} mode near 1058 cm^{-1} given by CH_3 rock/COH bend, and ν_{15} mode near 1066 cm^{-1} corresponding to the CO stretching. There is also one weaker ν_{10} mode of a *trans* ethanol centered at 1090 cm^{-1} that corresponds to the CO bond stretch vibration. Among these four fundamental modes, the ν_{15} mode of *gauche* ethanol is predominantly an a-type vibration, while the other three modes in this region are hybrid a/b-type (~2:1 ratio).

On the higher frequency end of our spectrum (Fig. 4c), we identified one strong ν_9 mode of the *trans* ethanol, which is a hybrid a/b-type (~1:1 ratio) absorption band centered at 1241 cm^{-1} and corresponding to the COH bending vibration. Here, there is also one weaker ν_{13} mode of the *gauche* ethanol near 1249 cm^{-1}, which is predominantly an a-type vibration corresponding to CH_2 twist.

3.3. Isoprene (C_5H_8)

The spectrum of gaseous isoprene was measured at two different conditions. In the first case (Fig. 5), we took an overview spectrum at a pressure of $p = 4$ mbar, the optical cavity length of 21 cm, spectral range 700–1075 cm^{-1} with interleaving 5 gradually shifted comb-mode-resolved spectra (spectral data point spacing 16 MHz). In the second case (Fig. 6), the spectrum was measured at $p = 0.185$ mbar, optical cavity length of 10.5 m, spectral range 800–1300 cm^{-1} with interleaving 7 spectra (data point spacing 11.4 MHz). For each measurement in both cases, we coherently averaged $N = 1000{,}000$ interferograms. For the future study, these data might be useful to model the c-type rovibrational bands associated with out-of-plane methylenic bending modes in the 800–1200 cm^{-1} region [25].

To identify absorption bands for isoprene, we followed the same assignments that were used in [10] taken primarily from [27]. The planar *s-trans* configuration of isoprene has a C_S point group symmetry, so it supports A' and A" symmetry modes. Here, we observe mostly A" fundamental modes that have c-type bands, and it is seen on the Figs. 5,6 where most of the bands look very similar. However, there are two A' symmetry modes near 994 cm^{-1} and 1071 cm^{-1} that will be mentioned below. On the Fig. 5, we have the weakest absorption band that we could observe in this region, which corresponds to the ν_{29} $=C1H_2$ twisting vibration and centered near 758 cm^{-1}. In the next measurement, presented on the Fig. 6, we focused on a high-frequency side of our spectrum with stronger bands of isoprene. A pair of closely spaced Q branches near 900 cm^{-1} belongs to the strongest isoprene absorption bands in the Mid-IR region, and it is an ideal candidate to serve as a spectral signature in atmospheric monitoring [10], or medical breath analysis. These bands are given by ν_{28} $C1H_2$ wag and ν_{27} $C4H_2$ wag centered near 894 cm^{-1} and 906 cm^{-1}, respectively. Further on the spectrum, we observed the ν_{26} fundamental mode centered at 992 cm^{-1} corresponding to the C3-H6 wagging vibration. Right next to it, there is a much weaker hybrid a/b-type band near 994 cm^{-1} of the ν_{17} $=C1H_2$ rocking vibration mode. Finally, in the region around 1070 cm^{-1}, we observe two absorption bands closely spaced to each other. The weaker absorption band centered at 1069 cm^{-1} is given by the ν_{25} asymmetric CH_3 rocking vibration mode, and the stronger hybrid a/b-type band near 1071 cm^{-1} correspond to the ν_{16} symmetric CH_3 rocking vibration mode.

3.4. DMS ($(CH_3)_2S$)

The absorption spectrum of gaseous DMS was measured at a pressure of $p = 2$ mbar and the optical cavity length of 238 cm. The spectrum (Fig. 7) was acquired by interleaving 6 gradually shifted comb-mode-resolved spectra resulting in an effective data point spacing of 13.3 MHz. We coherently averaged $N = 500{,}000$ interferograms for each spectrum. A few narrow absorption lines between 1350 and 1500 cm^{-1}, caused by trace amounts of water present in the optical gas cell, were manually excluded from the spectrum; the affected sections were replaced with straight lines to maintain continuity. Of particular interest is the use of these data to model the a/b/c-type methyl rocking rovibrational bands of DMS at 900–1100 cm^{-1} [25].

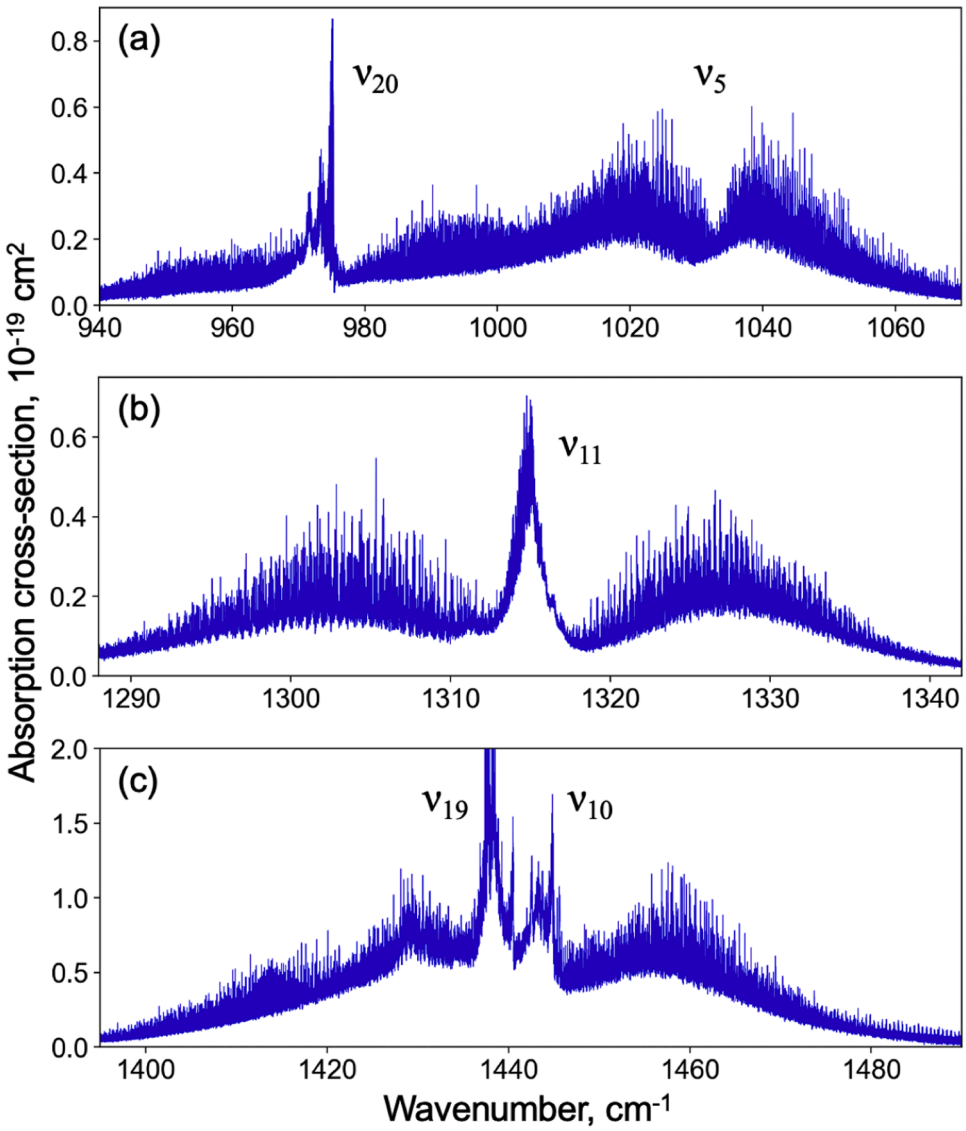

Fig. 8. Portions of absorption cross-section spectrum of DMS with mode assignments.

The DMS molecule has a C_{2V} point group, so it supports A_1, B_1, and B_2 symmetry modes, which give a rise to b-, a-, and c-type absorption bands, respectively. For DMS, we used mode assignments and descriptions of molecular motion involved in the fundamental vibration that was made from comparison with density functional (B3LYP/6-311+g(d,p)) calculations provided by Prof. David Nesbitt (University of Colorado Boulder). Zoomed-in portions of the spectrum with assignment of fundamental vibrational modes are shown in Fig. 8.

On the lower frequency end of our spectrum (Fig. 8a), we observe two absorption bands merging together. One band near 973 cm^{-1} has a distinctive Q branch of a B_2 symmetry c-type band, given by a symmetric CH_2 rocking vibration ν_{20}. The absorption band centered at 1030 cm^{-1}, displays the characteristic vibrational band contour without the Q branch given by an A_1 symmetry b-type band. This band is assigned to the ν_5 mode and corresponds to the symmetric CH wagging vibration.

On the higher frequency end of our spectrum, there is a well isolated from other vibrational modes the B_1 symmetry a-type rovibrational band at 1315 cm^{-1} (Fig. 8b), which is assigned to ν_{11} and given by antisymmetric CH_3 'umbrella' bend. In the 1440 cm^{-1} region (Fig. 8c), there are two closely spaced bands. One of them is centered around 1439 cm^{-1} and has a very strong Q branch (cropped on the Fig.) of a B_2 symmetry c-type absorption band, corresponding to the symmetric CH wagging vibration of a ν_{19} mode. Another absorption band of the a-type B_1 symmetry is centered near 1442 cm^{-1}, which is assigned to the ν_{10} mode and given by an asymmetric CH_2 bend.

4. Experimental data accuracy

The high absolute frequency accuracy in our MIR dual-comb spectroscopy system was achieved by stabilizing both driving Cr:ZnS laser combs through (i) phase-locking their carrier-envelope offset frequencies, and (ii) optically locking the comb teeth of the second harmonics of both lasers to a common narrow-linewidth (10 Hz) continuous-wave (CW) 1064-nm reference laser (Time-Base, Germany) that was frequency-stabilized using a high-finesse ultra-stable Fabry-Perot cavity made from ultra-low expansion glass and housed in a thermally stabilized vacuum chamber. Since all system frequencies, including the repetition rates of both lasers, the beat notes between the comb teeth and the reference CW laser, and the timing of the data acquisition card were referenced to a Rb atomic clock with a fractional uncertainty of 10^{-10}, the absolute frequency uncertainty did not exceed a few kHz ($\sim 10^{-7}$ cm^{-1}). Given the sub-kHz comb linewidths, the interleaving technique offers the potential for spectral resolution on a similar scale. The accuracy of the measured absorption cross-sections is

primarily limited by the purity of the analytical gas samples, the accuracy of gas cell length and pressure measurements, and the constancy of the pressure during spectral data collection. Taking all these factors into account, we estimate the overall fractional uncertainty in absorption cross-sections to be approximately 3–5 %.

5. Conclusion

Using an advanced dual-frequency-comb laser spectroscopy combined with electro-optic sampling, and with the absolute frequency referencing to an atomic clock, we performed broadband (700–1500 cm^{-1}), high-resolution (8–16 MHz, 0.00027–0.00053 cm^{-1}) spectral measurements of rovibrational transitions in gaseous methanol, ethanol, isoprene, and dimethyl sulfide. These measurements refined the absorption spectrum of methanol (CH_3OH) and revealed previously unobserved fine structure of the spectra of ethanol (C_2H_5OH), isoprene (C_5H_8), and dimethyl sulfide ($(CH_3)_2S$) in the above range. The resulting high-resolution, high-precision spectra represent the most comprehensive data to date and may aid in assigning rovibrational transitions and generating line lists for inclusion in HITRAN and similar databases.

CRediT authorship contribution statement

D. Konnov: Writing – review & editing, Visualization, Validation, Methodology. **A. Muraviev:** Writing – review & editing, Methodology, Investigation, Conceptualization. **K.L. Vodopyanov:** Writing – review & editing, Writing – original draft, Investigation, Funding acquisition, Conceptualization.

Declaration of competing interest

The authors declare that they have no known competing financial interests or personal relationships that could have appeared to influence the work reported in this paper.

Acknowledgments

We gratefully acknowledge Prof. David Nesbitt (University of Colorado Boulder) for his invaluable guidance and numerous insightful discussions that greatly contributed to these experiments. This work was supported through funding from the US Office of Naval Research (ONR) award N00014–18–1-2176; US Air Force Office of Scientific Research (AFOSR) awards FA9550–23–1-0126 and FA9550–24–1-0196; and U.S. Department of Energy, awards DE-SC0012704 and DE-FG02-09ER16021.

Data availability

Data will be made available on request.

References

[1] Xu LH, Lees RM, Wang P, Brown LR, Kleiner I, Johns JW. New assignments, line intensities, and HITRAN database for CH3OH at 10 μm. J of Mol Spectrosc 2004; 228:453–70.
[2] Gordon IE, Rothman LS, Hargreaves R, et al. The HITRAN2020 molecular spectroscopic database. JQSRT 2022;277:107949.
[3] Peters S, Semenov DA, Hochleitner R, et al. Synthesis of prebiotic organics from CO_2 by catalysis with meteoritic and volcanic particles. Sci Rep 2023;13:6843.
[4] Sharpe SW, Johnson TJ, Sams RL, Chu PM, Rhoderick GC, Johnson PA. Gas phase databases for quantitative infrared spectroscopy. J Appl Spectrosc 2004;58: 1452–61.
[5] Ding Y, Strand CL, Hanson RK. High-temperature mid-infrared absorption spectra of methanol (CH3OH) and ethanol (C2H5OH) between 930 and 1170 cm-1. JQSRT 2019;224:396–402.
[6] Seager S, Schrenk M, Bains W. An astrophysical view of earth-based metabolic biosignature gases. Astrobiology 2012;12(1):61–82.
[7] Zhan Z, Seager S, Petkowski JJ, Sousa-Silva C, Ranjan S, Huang J, Bains W. Assessment of isoprene as a possible biosignature gas in exoplanets with anoxic atmospheres. Astrobiology 2021;21:765–92.
[8] Mochalski P, King J, Mayhew CA, Unterkofler K. A review on isoprene in human breath. J. Breath Res. 2023;17:037101.
[9] Salerno-Kennedy R, Cashman KD. Potential applications of breath isoprene as a biomarker in modern medicine: a concise overview. Wien Klin Wochenschr 2005; 117:180–6.
[10] Brauer CS, Blake TA, Guenther AB, Sharpe SW, Sams RL, Johnson TJ. Quantitative infrared absorption cross sections of isoprene for atmospheric measurements. Atmos Meas Tech 2014;7:3839–47.
[11] Van den Velde S, Nevens F, van Steenberghe D, Quirynen M, analysis of breath odor compounds in liver patients GC–MS. J of Chromatography B 2008;875:344–8.
[12] Tangerman A, Winkel EG. Extra-oral halitosis: an overview. J of Breath Research 2010;4:017003.
[13] Jabri A, Belkhodja Y, Berger Y, Kleiner I, Asselin P. High resolution rovibrational analysis of dimethyl sulfide spectrum in the10 μm atmospheric window combining supersonic jet-quantum cascade laser and FTIR spectroscopies. J. of Mol. Spectrosc. 2018;349:32–6.
[14] Picqué N, Hänsch TW. Frequency comb spectroscopy. Nature Photon 2019;13: 146–57.
[15] Muraviev AV, Smolski VO, Loparo ZE, Vodopyanov KL. Massively parallel sensing of trace molecules and their isotopologues with broadband subharmonic mid-infrared frequency combs. Nature Photon 2018;12:209–14.
[16] Benea-Chelmus I-C, Faist J, Leitenstorfer A, Moskalenko AS, Pupeza I, Seletskiy DV, Vodopyanov KL. Electro-optic sampling of classical and quantum light. Optica 2025;12:546–63.
[17] Kowligy AS, Timmers H, Lind AJ, Elu U, Cruz FC, Schunemann PG, Biegert J, Diddams SA. Infrared electric field sampled frequency comb spectroscopy. Sci Adv 2019;5:eaaw8794.
[18] Konnov D, Muraviev A, Vasilyev S, Vodopyanov KL. High-resolution frequency-comb spectroscopy with electro-optic sampling and instantaneous octave-wide coverage across MIR to THz at a video rate. APL Photonics 2023;8:110801.
[19] Vasilyev S, Muraviev A, Konnov D, Mirov M, Smolski V, Moskalev I, Mirov S, Vodopyanov KL. Longwave infrared (6.6–11.4 μm) dual-comb spectroscopy with 240,000 comb-mode-resolved data points at video rate. Opt Lett 2023;48:2273–6.
[20] Vasilyev S, Moskalev IS, Smolski VO, Peppers JM, Mirov M, Muraviev AV, Zawilski K, Schunemann PG, Mirov SB, Vodopyanov KL, Gapontsev VP. Super-octave longwave mid-infrared coherent transients produced by optical rectification of few-cycle 2.5-μm pulses. Optica 2019;6:111–4.
[21] Muraviev AV, Konnov D, Vodopyanov KL. Broadband high-resolution molecular spectroscopy with interleaved mid-infrared frequency combs. Sci Rep 2020;10: 18700.
[22] Tran DBA, et al. Near- to mid-IR spectral purity transfer with a tunable frequency comb: methanol frequency metrology over a 1.4 GHz span. APL Photon 2024;9: 030801. https://doi.org/10.1063/5.0170227.
[23] Santagata R, et al. High-precision methanol spectroscopy with a widely tunable SI-traceable frequency-comb-based mid-infrared QCL. Optica 2019;6:411–23.
[24] Sun Z-D, et al. Dual-mode CO_2-laser/microwave-sideband spectrometer with broadband and saturation dip detection for CH_3OH. Rev Sci Instrum 2004;75: 1051–60.
[25] Nesbitt D, Chan Y-C, Temelkova EL, Konnov D, Muraviev A, Vodopyanov KL. Application of broad band dual frequency-comb methods to high resolution molecular spectroscopy in the THz to Mid IR frequency range for species relevant to terrestrial and exoplanetary atmospheres. In: Proceedings of the 77th Int. Symp on Molec Spectrosc; 2024. P7799. June 17-21paper.
[26] Durig JR, Deeb H, Darkhalil ID, Klaassen JJ, Gounev TK, Ganguly A. The r0 structural parameters, conformational stability, barriers to internal rotation, and vibrational assignments for trans and gauche ethanol. J of Mol Struct 2011;985: 202–10.
[27] Panchenko YN, Bock CW, Larkin JD, Abramenkov AV, Kühnemann F. Predictive abilities of scaled quantum-mechanical molecular force fields: application to 2-methylbuta-1, 3-diene (isoprene). Struct Chem 2008;19:421–8.